



Published in final edited form as:

*J Comput Phys.* 2012 June 1; 231(15): 5062–5077. doi:10.1016/j.jcp.2012.04.006.

## A Robust and Efficient Method for Steady State Patterns in Reaction-Diffusion Systems

Wing-Cheong Lo<sup>a,b,c,d</sup>, Long Chen<sup>a,b,c</sup>, Ming Wang<sup>a,e</sup>, and Qing Nie<sup>a,b,c</sup>

<sup>a</sup>Departments of Mathematics, University of California, Irvine, CA, USA

<sup>b</sup>Center for Complex Biological Systems, University of California, Irvine, CA, USA

<sup>c</sup>Center for Mathematical and Computational Biology, University of California, Irvine, CA, USA

<sup>d</sup>Mathematical Biosciences Institute, The Ohio State University, OH, USA

<sup>e</sup>LAMA, School of Mathematical Sciences, Peking University, Beijing, China

### Abstract

An inhomogeneous steady state pattern of nonlinear reaction-diffusion equations with no-flux boundary conditions is usually computed by solving the corresponding time-dependent reaction-diffusion equations using temporal schemes. Nonlinear solvers (e.g., Newton's method) take less CPU time in direct computation for the steady state; however, their convergence is sensitive to the initial guess, often leading to divergence or convergence to spatially homogeneous solution. Systematically numerical exploration of spatial patterns of reaction-diffusion equations under different parameter regimes requires that the numerical method be efficient and robust to initial condition or initial guess, with better likelihood of convergence to an inhomogeneous pattern. Here, a new approach that combines the advantages of temporal schemes in robustness and Newton's method in fast convergence in solving steady states of reaction-diffusion equations is proposed. In particular, an adaptive implicit Euler with inexact solver (AIIE) method is found to be much more efficient than temporal schemes and more robust in convergence than typical nonlinear solvers (e.g., Newton's method) in finding the inhomogeneous pattern. Application of this new approach to two reaction-diffusion equations in one, two, and three spatial dimensions, along with direct comparisons to several other existing methods, demonstrates that AIIE is a more desirable method for searching inhomogeneous spatial patterns of reaction-diffusion equations in a large parameter space.

### Keywords

Reaction-Diffusion; Steady State; Patterns; Hybrid Methods

### 1. Introduction

Reaction-diffusion equations are often used to model interactions among molecules and chemical species through reactions and random motion by diffusion [1, 2, 3, 4, 5, 6]. A reaction-diffusion system usually takes the form

© 2012 Elsevier Inc. All rights reserved.

**Publisher's Disclaimer:** This is a PDF file of an unedited manuscript that has been accepted for publication. As a service to our customers we are providing this early version of the manuscript. The manuscript will undergo copyediting, typesetting, and review of the resulting proof before it is published in its final citable form. Please note that during the production process errors may be discovered which could affect the content, and all legal disclaimers that apply to the journal pertain.

$$\frac{\partial u}{\partial t} = \mathcal{D}\Delta u + \mathcal{F}(u), \quad (1)$$

where  $u \in \mathbf{R}^m$  represents concentration of  $m$  types of molecules or chemical species,  $\mathcal{D} \in \mathbf{R}^{m \times m}$  is the matrix of diffusion coefficients, and  $\mathcal{F} \in \mathbf{R}^m$  represents reactions and interactions among different species.

The boundary conditions for (1) are critical in determining the property of reaction-diffusion equations. For example, when influxes of molecules or chemical species are from part of the domain, spatially inhomogeneous solutions and steady state patterns arise naturally due to the boundary conditions [7, 8]. For many applications, the boundary conditions are no-flux or periodic in every direction of regular domain [2, 3, 4, 5, 6]. For such homogeneous boundary conditions, some constants in space can be a steady state solution of the system; however, the interest of study is usually spatially inhomogeneous patterns in steady state that arise from a close interaction between reaction and diffusion, such as Turing patterning [9]. One major mechanism which consists of a short-range activation for the activator and a long-range inhibition for the inhibitor (drastic differences between the diffusion constants for the activator and the inhibitor) is responsible for spontaneous formation of many patterns in systems ranging from cell polarization [10, 11] to animal coats [12, 4].

To study the reaction-diffusion equations with homogeneous boundary conditions, such as no-flux boundary conditions, linear stability analysis around the spatially homogeneous steady state can provide necessary conditions and constraints on the parameters that allow pattern formation [9]. Other analytical theories, such as weakly nonlinear analysis [13], have been utilized for deriving more information on the specific form and stability of patterns [14, 15]. For complex biological models involving more species along with strong nonlinear regulations, linear stability analysis and analytical study become increasingly challenging. It leads to difficulty of finding the parameter regions permitting interesting patterns or choosing appropriate initial conditions evolving to desirable patterns.

One approach for systematic exploration of parameter regions for steady state patterns of a reaction-diffusion system is to apply temporal algorithms to solve equation (1) with various initial conditions. Because of the temporal stability constraint due to diffusion and possible stiff reactions, many time steps are required to compute the long time behavior of the temporal systems to approximate the steady state within a reasonable error, even using many recently developed new algorithms that are specifically designed to handle the stability constraints in diffusion [16, 17] and stiff reactions [17, 18, 19, 20]. In addition, one may need to search a large parameter space of the reaction-diffusion equation to find a correlation between parameters, which connect to specific biological processes, and patterns, which correspond to phenotypes [2, 21, 6].

Here, we focus on computing the steady state of (1) directly by solving the following system of equations

$$\mathcal{D}\Delta u + \mathcal{F}(u) = 0, \quad (2)$$

with no-flux boundary conditions. Note that a solution uniform in space (often called a homogeneous or constant solution) of the algebraic equation  $\mathcal{F}(u) = 0$  is also a solution to (2). Here, the goal of solving (2) is to identify non-constant solutions, corresponding to inhomogeneous spatial patterns.

One popular approach is to first approximate the differential operator in (2) to form a nonlinear algebraic system (e.g., through the finite difference method or the finite element method), and then solve the resulting nonlinear equations using Newton's method [22] or nonlinear multigrid methods [23, 24, 25]. Because of their strong dependence on the initial guesses, these types of iterative methods may easily converge to constant solutions of the algebraic equation  $\mathcal{F}(u) = 0$  even if the methods are efficient and convergent. For example, if the initial guess is not far from a homogeneous solution, Newton's method may converge to this solution even if it is unstable. While if using temporal schemes, perturbing from an unstable homogenous solution very likely leads to another stable solution, a possible spatial pattern. Our goal of solving (2) is to identify spatial patterns with minimal analytical knowledge of the solution, which is the case for most of the applications. Therefore, a desirable method needs to be efficient enough such that many parameters can be explored within a reasonable amount of time while the convergence to spatially inhomogeneous solutions is less sensitive to the choice of the initial guesses.

To this purpose, we present a hybrid approach that takes advantage of fast convergence of steady state solvers such as Newton's method and robustness of temporal schemes that usually always lead to a convergent solution. In particular, we apply the implicit Euler method to equation (1); however, without exactly solving the implicit equation during each time step, to generate a new iterative procedure for solving the equation (2). Several methods derived from this new approach are then applied to two different reaction-diffusion equations in one, two, and three spatial dimensions for a comparison with Newton's methods and some other existing methods. It is found that the new approach is much less sensitive to the initial guesses in generating spatially inhomogeneous solutions and is much more efficient than temporal schemes. Although the new iterative procedure might be slower in convergence than Newton's method, it is much more likely to converge to a spatial pattern for a given set of parameters. The balance of efficacy and robustness makes the new approach particularly suitable for computational searching of spatial patterns of reaction-diffusion equations in a large parameter space.

The paper is organized as follows. In section 2, we describe the new hybrid approach; in section 3, we compare several methods described in section 2 through two important performance measurements: likelihood of each method converging to spatially inhomogeneous steady state patterns and CPU time of convergence, for two reaction-diffusion equations in different spatial dimensions. In section 4, we conclude and discuss.

## 2. Methods

In this section, we first briefly describe three existing numerical methods: Newton's method, the implicit Euler method, and the FAS multigrid method, in a context of solving temporal or steady state reaction-diffusion equations. Following the description, we then present a new approach that integrates these three methods to solve the steady state equations (2).

To use Newton's method (**NM**) to solve the reaction-diffusion system (2), a spatial discretization of the linear diffusion operator usually leads to a nonlinear algebraic equation:

$$\mathbf{G}(u) = \mathbf{B}(u) + \mathbf{F}(u) = 0, \quad (3)$$

where  $\mathbf{B}$  is a discretized linear diffusion operator (e.g., through a second-order central difference scheme [26]) and  $\mathbf{F}$  is a nonlinear reaction term. In general,  $\mathbf{G}$  is a nonlinear function from  $\mathbf{R}^M \rightarrow \mathbf{R}^M$  with  $u \in \mathbf{R}^M$ , where  $M$  is the total number of unknowns. For example,  $M = mN$  for a one-dimensional  $m$ -variable system which is discretized in  $N$  spatial grid points. The Newton's iteration for (3) becomes

$$\mathbf{u}_{n+1} = \mathbf{u}_n - \mathbf{G}'(\mathbf{u}_n)^{-1} \mathbf{G}(\mathbf{u}_n). \quad (4)$$

It converges quadratically to a solution if the initial guess is close enough [22].

The implicit Euler method (**IE**) is an implicit time-evolution method for solving temporal reaction-diffusion systems with stiff reactions. IE takes the general form of

$$\frac{\mathbf{u}_{n+1} - \mathbf{u}_n}{\Delta t} = \mathbf{G}(\mathbf{u}_{n+1}). \quad (5)$$

The temporal solution  $\mathbf{u}_{n+1}$  is updated by the previous time step solution  $\mathbf{u}_n$  in an implicit form. When the sequence  $\mathbf{u}_n$  is convergent, it will converge to a stable solution of the steady state reaction-diffusion systems.

The main computational expense of the IE method is to solve the nonlinear system (5) for  $\mathbf{u}_{n+1}$  at each time step. Although IE is linearly absolutely stable allowing a large time step size  $\Delta t$  for stability reason [27], solving one nonlinear system at each time is still very expensive. In particular, the reaction-diffusion system needs to be solved for a large number of  $n$  to approach a steady state solution. Recall that our goal is to obtain approximation of steady state solutions (i.e., one only needs to derive an approximated solution  $\hat{\mathbf{u}}$ , such that  $\mathbf{G}(\hat{\mathbf{u}})$  is close to zero). As a result, the nonlinear system (5) does not need to be solved accurately at each time step.

### 2.1. Adaptive Implicit Euler Method with Inexact Solver (AIIE)

We present a new approach that uses only one Newton's iteration to solve the nonlinear system (5). Specifically, replacing  $\Delta t$  with  $\alpha$  in (5) and applying one Newton iteration with the initial guess  $\mathbf{u}_n$  yields this iteration procedure:

$$\mathbf{u}_{n+1} = \mathbf{u}_n - (\mathbf{G}'(\mathbf{u}_n) - \alpha^{-1} \mathbf{I})^{-1} \mathbf{G}(\mathbf{u}_n), \quad (6)$$

where  $\mathbf{I}$  is an identity matrix with the same dimension as  $\mathbf{G}'(\mathbf{u}_n)$ . We assume  $\alpha$  is chosen such that the operator  $\mathbf{G}'(\mathbf{u}_n) - \alpha^{-1} \mathbf{I}$  is non-singular. Clearly,  $\mathbf{G}(\mathbf{u}_{n+1})$  converges to zero as  $\mathbf{u}_{n+1}$  converges to a finite value in (6).

It is noted that the iterative procedure (6) is similar to a modified Newton's method [28]. The modification for the Newton's method in searching optimal points is mainly for the purpose of stabilizing the Jacobian matrix to improve the convergence property of Newton's method [29, 30]. Here, we dynamically vary the critical parameter  $\alpha$  to adjust the contribution of the temporal scheme and Newton's iteration such that the new method can exhibit advantages of both the temporal scheme and Newton's method.

We define this iteration procedure (6) as the inexact implicit Euler (**IIIE**) method. In IIIE, the intermediate solution  $\mathbf{u}_{n+1}$  is no longer an accurate approximation of the original temporal solution at  $t_{n+1}$ . If the nonlinear system (5) can be solved accurately using one Newton's iteration with the solution at the previous time step as the initial guess (this may be the case when  $\alpha$  is very small), the method (6) behaves similarly to an implicit Euler method.

For larger  $\alpha$ , to approximate the rate of convergence, we consider the extra term  $\alpha^{-1} \mathbf{I}$  as the error term of the Jacobian matrix approximation and apply the following theorem in [22].

**Theorem 1**—If  $G'$  is Lipschitz continuous and nonsingular at  $u = u^*$  where  $G(u^*) = 0$ , then there are  $C > 0$ ,  $\delta > 0$  and  $\delta_1 > 0$  such that if  $\|u_n - u^*\| < \delta$  and  $\|\mathbf{M}\| < \delta_1$  then

$$\mathbf{u}_{n+1} = \mathbf{u}_n - (\mathbf{G}'(\mathbf{u}_n) - \mathbf{M})^{-1} \mathbf{G}(\mathbf{u}_n),$$

is defined and satisfies

$$\|\mathbf{u}_{n+1} - \mathbf{u}^*\| \leq C(\|\mathbf{u}_n - \mathbf{u}^*\|^2 + \|\mathbf{M}\| \|\mathbf{u}_n - \mathbf{u}^*\|).$$

If the initial guess for (6) is close to the steady state solution, denoted as  $\mathbf{u}^*$ , we let  $\mathbf{M} = \alpha^{-1} \mathbf{I}$  ( $\|\mathbf{M}\| = \|\alpha^{-1} \mathbf{I}\| = \alpha^{-1}$ ) and apply Theorem 1 to obtain

$$\|\mathbf{u}_{n+1} - \mathbf{u}^*\| \leq C(\|\mathbf{u}_n - \mathbf{u}^*\|^2 + \alpha^{-1} \|\mathbf{u}_n - \mathbf{u}^*\|), \quad (7)$$

where  $C$  is a positive number independent of  $n$ . As seen in (7), when  $\alpha$  is very large, the iterative procedure behaves similarly to Newton's method with a quadratic convergence rate.

Similar to temporal schemes with an adaptive time step, an adaptive  $\alpha$  presumably makes the iteration process of (6) more robust and efficient. We denote IIE with an adaptive  $\alpha$  as **AIIE**. When  $\alpha$  is small, the nonlinear system (5) can be solved accurately using one Newton's iteration with the solution at the previous time step so AIIE behaves similarly to an implicit Euler method. Note that when  $\alpha \rightarrow 0$ , the iteration process of (6) also approaches to an explicit Euler method. In (6), the term  $-(\mathbf{G}'(\mathbf{u}_n) - \alpha^{-1} \mathbf{I})^{-1} \mathbf{G}(\mathbf{u}_n)$  can be rewritten as

$$-(\mathbf{G}'(\mathbf{u}_n) - \alpha^{-1} \mathbf{I})^{-1} \mathbf{G}(\mathbf{u}_n) = (\mathbf{I} + \alpha \mathbf{G}'(\mathbf{u}_n) + \alpha^2 \mathbf{G}'(\mathbf{u}_n)^2 + \dots) \alpha \mathbf{G}(\mathbf{u}_n).$$

When  $\alpha \rightarrow 0$ , it equals to  $\alpha \mathbf{G}(\mathbf{u}_n)$  after skipping all the higher order terms. So (6) becomes

$$\mathbf{u}_{n+1} = \mathbf{u}_n + \alpha \mathbf{G}(\mathbf{u}_n),$$

which equals to a time update process of an explicit Euler method. It is consistent that when  $\alpha$  is small, the difference between  $\mathbf{u}_{n+1}$  and  $\mathbf{u}_n$  is small so implicit Euler method behaves like explicit Euler method.

When  $\alpha$  is large, according to (7), AIIE behaves more similarly to Newton's method, which has a quadratic convergence rate.

To take advantage of both NM and IE, we choose to increase  $\alpha$  in IIE adaptively for an adaptive IIE (AIIE) such that the overall method gradually switches from a temporal scheme to a steady state solver like Newton's method during the iteration process. Typically,  $\alpha$  is chosen to be an increasing function of  $n$ , such as  $\alpha = 0.1n$ ,  $\alpha = 2n$  and  $\alpha = n$ , as shown in the next section for direct numerical tests. Among those three choices, it is found for the reaction-diffusion equations tested in this paper that  $\alpha = n$  provides the best performance and robustness for AIIE.

## 2.2. FAS Multigrid Method with AIIE (FAIIE)

The nonlinear multigrid methods [23, 24] can enable rapid convergence by employing grids of different mesh size in solving nonlinear systems. Through a suitable smoothing operator and coarse grid correction, a multigrid approach can accelerate convergence, particularly for diffusion-dominated systems in multi-spatial dimensions. Here, we integrate a Full-Approximation Storage (FAS) multigrid method with the new AIIE approach, denoted as FAIIE, to solve the system (3) using a two-grid iteration cycle [23, 24]. Here is an outline of the iteration procedure:

1. Obtain an approximation  $\mathbf{v}^h$  by performing  $n_1$  times AIIE iteration on  $\mathbf{G}^h(\mathbf{u}^h) = 0$ .
2. Restrict the approximation  $\mathbf{v}^h$  and its residual to the coarse grid:

$$\mathbf{v}^{2h} = I_h^{2h} \mathbf{v}^h, \quad \mathbf{r}^{2h} = I_h^{2h} (-\mathbf{G}^h(\mathbf{v}^h)).$$

3. Smooth  $n_2$  times AIIE iteration on the coarse-grid residual problem:

$$\mathbf{G}^{2h}(\mathbf{u}^{2h}) = \mathbf{G}^{2h}(\mathbf{v}^{2h}) + \mathbf{r}^{2h}.$$

4. Extract the coarse-grid correction:  $\mathbf{e}^{2h} = \mathbf{u}^{2h} - \mathbf{v}^{2h}$ .
5. Interpolate and apply the correction:  $\mathbf{v}^h = \mathbf{v}^h + I_{2h}^h \mathbf{e}^{2h}$ .

Similar to AIIE,  $\alpha$  can be adjusted according to the number of FAS iterations. In this paper, we set  $n_1 = n_2 = 1$  and only consider FAIIE with  $\alpha = n$ , where  $n$  is the number of iteration cycles of the FAS method.

The performance of the FAS multigrid method depends crucially on a smoother and a coarse grid solver, and nonlinear Gauss-Seidel smoother usually is used for a typical FAS multigrid approach. In the numerical tests shown in the next section, it is found that the FAS multigrid with a Gauss-Seidel nonlinear smoother typically results in divergence or convergence to a homogeneous solution, showing no interesting biological patterns. With AIIE as a smoother, the overall method more likely converges to an inhomogeneous solution with spatial pattern. For the rest of the paper, we choose AIIE as a smoother for the FAIIE approach. We note that if the inverse  $(\mathbf{G}'(\mathbf{u}_n) - \alpha^{-1}\mathbf{I})^{-1}$  in AIIE is computed by a direct solver, smoother calculation is not cheap. However, here we keep such structure of FAS and leave the investigation of a more efficient smoother to future work.

## 3. Numerical Results

Our interest is to find all types of inhomogeneous solutions with a spatial pattern of reaction-diffusion system. Therefore, an important performance measurement for a nonlinear solver is the robustness of converging to inhomogeneous solutions. How sensitively a method depends on its initial guesses to produce a spatially inhomogeneous solution becomes critically important. Therefore, in addition to comparing efficiency, which is measured as CPU time for obtaining a solution, we also focus on studying the likelihood of each numerical method converging to spatially inhomogeneous steady state patterns.

In this section, we first consider two reaction-diffusion biological models in one spatial dimension for five different numerical methods: Newton's method (NM), Implicit Euler (IE), Implicit Euler with inexact nonlinear solver (IIE), IIE with adaptive  $\alpha = n$  (AIIE), and FAS on IIE (FAIIE) with adaptive  $\alpha = n$ , as described in the previous section. Next, we extend our study of NM and AIIE to two-dimensional and three-dimensional domains to

show that the results are consistent with the one-dimensional examples. We finally study how the performances of NM and AIIE depend on the number of spatial grid points. All the numerical tests are implemented in MATLAB with the help of the software package iFEM [31]. For solving the linear system in (4) or (6), it is found that the Gauss-Seidel method and the multigrid method with a Gauss-Seidel smoother usually results in non-convergence. In this paper, we solve the linear system by using the direct solver built in MATLAB. The numerical parameter settings will be discussed in the later sections.

### 3.1. One-dimensional systems

Here, we study all five methods under two possible scenarios depending on how much analytical information can be obtained for the reaction-diffusion equations. The first scenario is when the linear stability analysis around the homogeneous steady state solutions can be carried out analytically to obtain a set of necessary conditions for parameters resulting in inhomogeneous patterns. For this case, we study how the convergence of each method to inhomogeneous patterns depends on the initial guess, which is chosen as a perturbation from the homogeneous steady state solution. The second scenario is when no analytical information of the reaction-diffusion equation is known. For this case, we compare the five methods using a large set of randomly chosen initial guesses and parameters to study performance in terms of robustness and efficiency.

**3.1.1. A system with linear stability analysis and known homogeneous solutions**—The normalized one-dimensional activator-substrate system [32] has the following form:

$$\begin{cases} \frac{\partial A}{\partial t} = D\Delta A + SA^2 - A + \rho, \\ \frac{\partial S}{\partial t} = \Delta S + \mu(1 - SA^2), \end{cases} \quad (8)$$

in  $x \in (0, 10)$  with no-flux boundary conditions at both ends. The substrate  $S$  may be depleted by activator  $A$ . The constant  $D$  measures the diffusion coefficient ratio of activator to substrate. The parameters  $\rho$  and  $\mu$  measure the production rates of activator and substrate, respectively.

Solving the system

$$\begin{cases} SA^2 - A + \rho = 0, \\ \mu(1 - SA^2) = 0, \end{cases} \quad (9)$$

gives us a homogeneous steady state:

$$A^* = 1 + \rho, \quad S^* = (1 + \rho)^{-2}. \quad (10)$$

The linear stability analysis in [32] states that an inhomogeneous steady state may exist if the following inequalities hold:

$$\mu \geq \frac{2}{1 + \rho} - 1, \quad \mu D < \left( \sqrt{\frac{2}{1 + \rho}} - 1 \right)^2. \quad (11)$$

In particular, we choose parameter ranges as

$$\rho \in (0, 1), \mu \in \left( \frac{2}{1+\rho} - 1, 2 \right), D \in \left( 0.001, \frac{1}{\mu} \left( \sqrt{\frac{2}{1+\rho}} - 1 \right)^2 \right). \quad (12)$$

The ranges in (12) give a subset of parameters satisfying the conditions (11) for the existence of inhomogeneous steady state patterns. The initial guess  $(A_0, S_0)$  takes the following form:

$$A_0 = A^*(1 + \gamma \delta_A(x)), \quad S_0 = S^*(1 + \gamma \delta_S(x)), \quad (13)$$

where  $\delta_A(x)$  and  $\delta_S(x)$  are standard normally distributed random variables with zero mean and variance being one. All of the random variables are spatially independent. The constant  $\gamma$  is used to measure the magnitude of the perturbation away from the homogeneous solution  $(A^*, S^*)$ . Figure 1 is a typical inhomogeneous steady state pattern of equation (8).

To study how the convergence of each method to an inhomogeneous pattern depends on the initial guess (13) for different perturbation amplitude  $\gamma$ , we randomly select 100 sets of parameters from the analytically derived range (12) with uniform probability distribution. Then we investigate the percentage of such simulations converging to an inhomogeneous pattern and the average CPU time per simulation for obtaining the approximated solution.

Denote  $N = 2^J + 1$  as the number of spatial points where  $J$  is a positive integer. In Figure 2, we choose  $J = 10$ , and for NM, IIE ( $\alpha = 1, 10$ ), AIIE, FAIIE, the iteration is considered to converge to steady state if the residual in the form of (3) is less than  $10^{-7}$  within 1,000 iterations. For IE, the implicit equation (5) is solved by Newton's method with a tolerance of  $10^{-10}$ . In this paper, if we do not mention the number of spatial grid points, iteration tolerances and implementation, all of them are chosen to be the same as in Figure 2.

In the simulations for each  $\gamma$  with 100 sets of randomly generated parameters and initial guesses, all methods except IIE with  $\alpha = 1$  have more than 90% of the cases converging to either a homogeneous steady state or an inhomogeneous pattern. IIE with  $\alpha = 1$  has only around 30% of the cases converging within 1,000 iterations. With relatively small  $\alpha$ , IIE behaves like an implicit Euler method, as  $\alpha$  is similar to a time step, and most of the parameters make the IIE less "stable" with such a large "time step" leading to non-convergence.

Next we study the percentage of simulations that converge to inhomogeneous patterns and average CPU time used for simulating one set of parameters. As shown in Figure 2, the likelihood that NM will converge to inhomogeneous patterns strongly depends on  $\gamma$ , the size of perturbation in the initial guess. If the initial guess is closer to a homogeneous steady state, it is less likely that NM will converge to an inhomogeneous pattern. As expected, once convergence, NM costs the least average CPU time used for simulating one set of parameters.

On the other hand, the likelihood of convergence to inhomogeneous patterns for all four other methods seems to be insensitive to the perturbation parameter  $\gamma$  in the initial guess (13). This is not surprising because all of the four methods have some characteristics of temporal schemes and the iterated solutions evolve away from the unstable homogeneous solution. Among these four methods, AIIE has a similar likelihood of obtaining inhomogeneous patterns as IE, a temporal scheme which is most likely to obtain inhomogeneous patterns, while AIIE is the cheapest one in average CPU time per simulation and IE is significantly more expensive. The advantage of AIIE becomes clear among these four methods, as seen in Figure 2. FAIIE is a bit more expensive than AIIE. The



convergence of FAIIE is mainly due to AIIE, so there is no benefit from FAS. The results also show that IIE with a fixed  $\alpha$  is not as good as AIIE in CPU time as well.

Compared with AIIE, NM is much more likely to obtain homogeneous solutions for a very small  $\gamma$ , although NM is significantly cheaper in CPU for this case. On the other hand, for large  $\gamma$  (e.g., close to  $\gamma = 0.5$ ), the likelihood of obtaining inhomogeneous patterns for NM is just slightly smaller than for AIIE while the CPU time per simulation for NM is also only slightly better than AIIE for a large  $\gamma$ .

In short, there is a trade-off between robustness and efficiency, i.e., likelihood of obtaining inhomogeneous patterns and CPU time for NM and AIIE. To obtain inhomogeneous patterns, NM is much more sensitive to initial guess than AIIE while NM is cheaper once it converges. Of course, the details of such a trade-off are problem-dependent and vary from system to system.

### 3.1.2. A system without analytical information of the homogeneous steady state solution

—When the reaction term in a reaction-diffusion system takes general nonlinear function with saturations, such as the Hill function [4], or the system involves more than two equations, analytical information of the solution to the system becomes difficult to obtain. As an example, we consider another activator-substrate system [32] with Hill functions in the nonlinear reaction term:

$$\begin{cases} \frac{\partial A}{\partial t} = D\Delta A + \frac{SA^2}{1+A^2} - A + \rho \\ \frac{\partial S}{\partial t} = \Delta S + \mu \left(1 - \frac{SA^2}{1+A^2}\right), \end{cases} \quad (14)$$

in  $x \in (0, 10)$  with no-flux boundary conditions at both ends.

Following the same process as in subsection 3.1.1, we can still derive a homogeneous steady state of system (14):

$$A^* = 1 + \rho, \quad S^* = 1 + (1 + \rho)^{-2}. \quad (15)$$

However, in order to test the performance of all the methods when analytical information is not provided, we do not use the analytical information of the system (14). We search for inhomogeneous patterns by randomly sampling parameters within given ranges:

$$\rho \in (0, 1), \quad \mu \in (0, 2), \quad D \in (0.001, 0.1). \quad (16)$$

Specifically,  $\rho$  and  $\mu$  are uniformly selected in the range (16) and the probability distribution of  $D$  is log-uniform. The initial guesses have the following form:

$$A_0 = 1 + \gamma \delta_A(x), \quad S_0 = 1 + \gamma \delta_S(x), \quad (17)$$

where  $\delta_A(x)$  and  $\delta_S(x)$  are defined the same as in (13).

Similar to the study in the previous subsection, we select 1,000 sets of parameters for each  $\gamma$  with an initial guess in the form of (17) and compare NM, IIE ( $\alpha = 1, 10$ ), AIIE, FAIIE and IE with different values of  $\gamma$ . To ensure the sample size is large enough for statistically reliable results, we also double the sample size to 2,000 sets of parameters for each  $\gamma$  and find the results are consistent between the two kinds of sampling.

It is found that more than 90% of the simulations for each method converges to steady state solution. However, most of the convergent solutions are spatially homogeneous solutions, with about 2.5% of the convergent cases inhomogeneous at best. The result is understandable, since we do not have a priori information on the range of parameters to produce patterns. We verify that the steady state is an inhomogeneous pattern by checking if the diffusion term  $\mathbf{B}u$  is larger than  $10^{-4}$ ; this is also confirmed by observation.

As the results shown in Figure 3, the likelihood that NM will converge to inhomogeneous patterns strongly depends on  $\gamma$ , and NM costs the least average CPU time per simulation. This is consistent with what we observed in the previous subsection. For  $\gamma = 0.5$ , NM has a higher likelihood of obtaining inhomogeneous patterns than the other four methods. It is different from the results shown in Figure 2 that AIIE always has a higher likelihood of obtaining inhomogeneous patterns than NM.

Without considering the likelihood of obtaining inhomogeneous patterns, NM is the most efficient method among all the five methods. If the initial guess with suitable range of perturbation can be obtained, NM may be the most efficient and robust method. However, the process for searching a suitable range of perturbation may take significantly more CPU time, especially in two-dimensional and three-dimensional domains. If we require that the performance of the method has to be less sensitive to the initial guess, AIIE is the most efficient method for obtaining inhomogeneous patterns.

To further explore this observation, we study the performances of NM and AIIE by selecting parameters  $\rho$  and  $\mu$  in a uniform distribution of the ranges  $[0.001, 0.1]$  and  $[0.01, 1]$  respectively, with three different diffusion ratios  $D = 0.0005, 0.001$  and  $0.002$  using the initial guess of the form (17).

The choice of the parameter ranges is motivated by the results of Figure 3, in which most of the inhomogeneous patterns appear within the following parameter ranges:

$$\rho \in (0.001, 0.1), \quad \mu \in (0.01, 1), \quad D \in (0.001, 0.002). \quad (18)$$

For each set of parameters, NM and AIIE are carried out for both  $\gamma = 0.1$  (Figure 4) and  $\gamma = 0.5$  (Figure 5). For the case  $\gamma = 0.1$ , AIIE method leads to a wider white region than NM method (Figure 4), showing that AIIE is more likely to produce an inhomogeneous pattern than NM; when  $\gamma$  increases from 0.1 to 0.5, the white region for AIIE does not change much, while the white region obtained through NM is enlarged with increasing  $\gamma$ . The result on likelihood of converging to inhomogeneous patterns for both AIIE and NM, consistent with the case when parameters are randomly selected.

The average CPU times used for simulating one set of parameters using NM are 0.108s and 1.307s for the case  $\gamma = 0.1$  and the case  $\gamma = 0.5$ , respectively. The average CPU times used for simulating one set of parameters with AIIE are 2.528s and 3.865s for  $\gamma = 0.1$  and  $\gamma = 0.5$ , respectively. The average CPU time per simulation depends on  $\gamma$  because the time used for convergence is related to how close the initial guess is to the steady state. When  $\gamma = 0.1$ , the initial guess is close to the homogeneous steady state, NM converges to homogeneous steady state rapidly. When  $\gamma = 0.5$ , the initial guess is far from the homogeneous steady state but may not be close to the inhomogeneous one, so more CPU time is required.

The time cost per simulation is increasing when the diffusion ratio  $D$  is decreasing when applying NM and AIIE. For AIIE, there are more non-convergence cases when  $D$  decreases because the number of iterations for convergence is increasing per case (example in Figure 6). With a small  $D$ , the system is dominated by the nonlinear reaction term, leading to more

iterations for both AIIE and NM. AIIE becomes less effective as it is designed for a system with diffusion.

### 3.2. Two-dimensional and three-dimensional systems

We next study the performance of NM and AIIE for systems in two-dimensional and three-dimensional domains. In particular, we consider the system (14) in  $(x, y) \in (0, 2) \times (0, 2)$  and  $(x, y, z) \in (0, 10) \times (0, 10) \times (0, 10)$  with no-flux boundary conditions on all boundaries.

Similar to the one-dimensional tests,  $\rho$  and  $\mu$  are generated uniformly in the ranges [0.001, 0.1] and [0.01, 1] respectively, with fixed diffusion ratios  $D = 0.001$ . The initial guesses have the following forms:

$$2D: A_0 = 1 + \gamma \delta_{A2D}(x, y), \quad S_0 = 1 + \gamma \delta_{S2D}(x, y); \quad (19)$$

$$3D: A_0 = 1 + \gamma \delta_{A3D}(x, y, z), \quad S_0 = 1 + \gamma \delta_{S3D}(x, y, z), \quad (20)$$

where  $\delta_{A2D}(x, y)$ ,  $\delta_{S2D}(x, y)$ ,  $\delta_{A3D}(x, y, z)$  and  $\delta_{S3D}(x, y, z)$  are standard normally distributed random independent variables with zero mean and variance being one. For each set of parameters, NM and AIIE are carried out for  $\gamma = 0.1$  and  $\gamma = 0.5$  (Figures 7 and 8). The grid levels  $J$  are set to be 6 in the two-dimensional domain with a total number of spatial grid points  $N = (2^J + 1)^2$ ; for the three-dimensional domain, we set  $J = 4$  with the total number of grid points  $N = (2^J + 1)^3$ .

Figures 7 and 8 for the two- and three- dimensional systems exhibit similar behavior as that seen in the one-dimensional system in Figures 4 and 5. The performance of NM is more sensitive to the magnitude of perturbation acted on the initial guess than AIIE. From the point of view of CPU time, NM is more efficient than AIIE for one simulation. The overall performance of AIIE and NM for the two- and three-dimensional systems is consistent with that of the one-dimensional model (that is, AIIE is more robust in obtaining an inhomogeneous pattern, while NM is more efficient if it is convergent).

### 3.3. Spatial resolution refinement tests

To understand how the number of grid points affects convergence, we first study the performance of NM and AIIE using different spatial level  $J$  (number of spatial points  $N = 2^J + 1$ ) for the one-dimensional system (14) with initial guesses of form (17). Figure 9A shows that when  $J$  increases, the likelihood that NM will converge to inhomogeneous patterns is reduced. It is clear that the likelihood that NM will obtain inhomogeneous patterns is much more sensitive to the number of spatial grid points regardless of the size of perturbation acted on the initial guess. Compared with NM, the robustness of AIIE is slightly affected by the change of  $J$ , the spatial resolution.

In the case of Figure 9A, the initial guess for both methods is independent at each spatial resolution and is directly generated from the equation (17). The two methods behave differently if the initial guesses are generated by linearly interpolating the initial guesses on the coarse grid  $J = 6$  to the fine grids  $J = 8, 10, 12$  and  $14$  for their initial guesses. Figure 9B shows that the likelihood of NM and AIIE converging to inhomogeneous solutions is much less sensitive when the number of spatial grid points is varied.

The analysis of previous section shows that the likelihood of converging to inhomogeneous solutions increases when the magnitude of perturbation of the initial guess increases. The reason is that the amplitudes of non-zero frequencies of the perturbation increase with the magnitude of perturbation [33] and enough strength of some non-zero frequencies is

necessary for leaving a homogeneous steady state and converging to an inhomogeneous pattern [32, 9]. For the simulations in Figure 9B, the amplitudes of the frequencies of the perturbation are not affected during the spatial refinement because the initial guesses have the “same” form in different spatial levels. So the likelihood of NM and AIIE converging to inhomogeneous solutions is not affected by the spatial resolution. But for the simulations in Figure 9A, the increase of spatial levels may reduce the strength of some non-zero frequencies so there is not enough level of perturbation for a convergence to an inhomogeneous pattern. Then the likelihood of convergence to inhomogeneous solutions decreases when the spatial level increases.

Sometimes, although the change of spatial resolutions may not significantly affect the likelihood of convergence to inhomogeneous patterns, a specific form of pattern may be varied as the spatial level  $J$  changes. For some cases, the corresponding numerical method may not converge to the exact steady state solution of the continuous reaction-diffusion equations and the convergent solution for a fixed number of spatial grid points is only the steady state solution of the corresponding finite-dimensional discretized system.

To study how the pattern is varied as the spatial level  $J$  changes, we apply both AIIE and NM to the one-dimensional system (8) using 50 sets of parameters and initial guesses in the form (13). In all sets of the parameters and initial guesses, both NM and AIIE converge to inhomogeneous patterns using  $J=9$  level of grid. Here, the initial guesses are first generated for  $J=9$  coarse grid ( $N=2^J+1$ ) and are linearly interpolated to  $J=10$  level of grid. When the level of grid increases from  $J=9$  to  $J=10$ , AIIE maintains the same form of pattern in 46% of cases, while NM converges to the same form of pattern only in 16% of cases. In this test, AIIE is more likely to maintain the same of pattern during the spatial resolution than NM. Here two patterns are defined to be the same if their relative pointwise difference is less than 0.1%.

We further investigate this in two-dimensional systems. We apply AIIE and NM to different initial guesses using the two-dimensional system (14). The initial guesses are first generated for  $J=6$  coarse grid ( $N=(2^J+1)^2$ ) and they are then linearly interpolated to  $J=7$  and  $J=8$  level of grids.

Initial guesses for  $A$  or  $S$  of the system (14) in a two-dimensional domain are defined as follows:

$$\begin{aligned} IG1(\vec{x}) &= \begin{cases} \delta_U(\vec{x}) & \text{if } \vec{x} \in D_1; \\ 0 & \text{otherwise,} \end{cases} & IG3(\vec{x}) &= \begin{cases} \delta(\vec{x}) & \text{if } \vec{x} \in D_1; \\ 1 & \text{otherwise,} \end{cases} \\ IG2(\vec{x}) &= \begin{cases} \delta_U(\vec{x}) & \text{if } \vec{x} \in D_2; \\ 0 & \text{otherwise,} \end{cases} & IG4(\vec{x}) &= \begin{cases} \delta(\vec{x}) & \text{if } \vec{x} \in D_2; \\ 1 & \text{otherwise,} \end{cases} \\ & & IG5(\vec{x}) &= \delta(\vec{x}), \end{aligned}$$

where  $D_1 = \{(x, y) : |(x, y) - (5, 5)| < 2\}$ ,  $D_2 = \{(x, y) : |(x, y) - z \rightarrow| < 1, z \rightarrow = (3, 3), (3, 7), (7, 3), (7, 7)\}$ ,  $\delta_U(x)$  is a uniformly distributed random number in  $[0, 1]$  and  $\delta(x)$  is a normally distributed random variable with zero mean and 0.5 for its variance. The spatial patterns for those five initial guesses are shown in Figure 10.

In the test, we choose one set of parameters for each model. Time evolution simulation shows that the inhomogeneous steady state exists with this set of parameters. Figure 11 shows that AIIE and NM converge to inhomogeneous patterns in all simulations for  $J=6$ . To examine if those steady state patterns are locally stable for the corresponding temporal reaction-diffusion equation, we use a second-order Runge-Kutta method with an initial

condition that is perturbed away from the steady state  $(A^*, S^*)$  computed by AIIE or IE. In particular, the initial conditions with perturbation have the following form:

$$A_0 = (1 + 0.1\delta_A(x, y))A^*, \quad S_0 = (1 + 0.1\delta_S(x, y))S^*, \quad (21)$$

where  $\delta_A(x, y)$  and  $\delta_S(x, y)$  are standard normally distributed random independent variables with zero mean and variance being one. For a fixed spatial resolution, all temporal evolutions eventually go back to the steady state solution computed by AIIE or NM, showing the steady state solutions are locally stable for the finite discretized system. However, when the number of spatial points increases, all the convergent solutions using NM change to different patterns, with some cases failing to converge to an inhomogeneous pattern (e.g., IG3, Figure 11). Among the five initial conditions, only the case IG4 seems to show a consistent pattern when spatial resolution is varied. In contrast, when AIIE is used, the cases IG3, IG4 and IG5 all show a consistent pattern when the spatial resolution increases. AIIE seems to be more likely to maintain the same form of pattern during the spatial resolution, suggesting that the steady state solution of the discretization system is more likely to converge to the steady state of the continuous system.

To investigate if this property of AIIE and NM depends on a particular form of reaction-diffusion equations, we study another system, the Gray-Scott model [6] in a two-dimensional domain  $(x, y) \in (0, 10) \times (0, 10)$ :

$$\begin{cases} \frac{\partial A}{\partial t} = D_A \Delta A - AS^2 + \rho(1-A), \\ \frac{\partial S}{\partial t} = D_S \Delta S + AS^2 - (\rho+k)S, \end{cases} \quad (22)$$

which has no-flux boundary conditions on all edges of the domain. The model describes the growth of an activator  $A$  reacted with substrate  $S$  fed from the activator with a rate  $\rho$ , and  $S$  is converted to an inert product at the rate  $k$ .  $D_A$  and  $D_S$  are the diffusion coefficients of  $A$  and  $S$ , respectively.

Instead of producing the pattern of spots in Figure 11, the system (22) generates the stripe patterns shown in Figure 12. As expected, NM is unable to produce consistent patterns for either one of the five initial guesses when the spatial resolution increases; however, AIIE is able to produce a consistent stripe pattern for at least two out of the five initial guesses (e.g., IG1, IG2 in Figure 12).

We further study the effect of spatial resolution for the systems (14) and (22) in a three-dimensional domain  $(x, y, z) \in (0, 10) \times (0, 10) \times (0, 10)$  using three different initial guesses. The three initial guesses for  $A$  or  $S$  in a three-dimensional domain are the corresponding three-dimensional version of IG1, IG3, IG5, where  $D_1 = \{(x, y, z) : |(x, y, z) - (5, 5, 5)| < 2\}$ . The total number of spatial grid points for the three-dimensional system is  $N = (2^J + 1)^3$ .

For the system (22), NM converges to inhomogeneous patterns or homogeneous steady states on the grid level  $J = 3$ , but NM does not converge on the grid levels  $J = 4, 5$ . However, AIIE converges to steady state on all grid levels. All the steady states AIIE obtains on  $J = 4, 5$  are inhomogeneous patterns. Figure 13 shows the form of a three-dimensional pattern computed by AIIE using the initial guess IG1. The form of pattern is similar to that found in a two-dimensional domain.

For the system (14), AIIE and NM both converge to inhomogeneous patterns on the coarsest grid level  $J = 3$ . When the grid level increases to  $J = 4$  or  $5$ , both AIIE and NM do not converge to any steady state. Although both methods converge on the grid level  $J = 3$ , the

patterns obtained may not be the “real” patterns of the continuous reaction-diffusion equations due to the large error of spatial approximation. On the finer grids  $J = 4, 5$ , AIIE and NM are unable to converge to any steady state solution. This is probably due to the fact that the initial guesses are far from any steady state, suggesting that better initial guesses may be needed for both methods to converge in three dimensions.

In general, AIIE is found to be relatively more consistent in generating the same pattern when the spatial resolution is refined. NM may converge in low spatial resolution; however, it may lose convergence in a higher spatial resolution. Also, a convergent pattern computed by NM to solve the same system is more likely to vary when its spatial resolution is varied.

#### 4. Conclusion and Future Work

In this paper, we have presented a new hybrid approach to solve steady states of reaction-diffusion equations with no-flux boundary conditions. AIIE, one of the new methods, integrates the implicit Euler temporal scheme with one Newton iteration. This method behaves similarly to a temporal scheme during the early part of the iteration process and gradually becomes a Newton’s method as iteration continues. The design principle of this method is to take advantage of strengths in both an implicit temporal scheme, which is robust in finding steady state inhomogeneous solutions, and Newton’s method, which has a fast convergence when the method does converge.

For most existing numerical methods, a trade-off usually occurs between the likelihood of finding an inhomogeneous pattern and CPU time for a method to converge. AIIE seems to alleviate such a trade-off to a certain degree. AIIE is faster than the temporal schemes, while its convergence to a spatially inhomogeneous pattern is less sensitive to initial guess and spatial grid size compared with Newton’s method. In other words, AIIE may be the most efficient, compared with existing methods, in searching for spatial inhomogeneous patterns. Because each simulation for a given set of parameters may diverge or converge to a spatially homogeneous solution, the efficiency of such a task is determined by two factors: likelihood of converging to patterns and CPU time for each convergent simulation. Therefore, an efficient method for finding patterns needs a balance of performances affected by these two factors.

Although AIIE is shown to have good performance and efficiency, several improvements can be made for the new approach introduced in this paper. The dominant cost of AIIE, similar to Newton’s method, comes from solving the linear system involving the Jacobian matrix at each iteration step. Since the Jacobian matrix in (4) or (6) is tridiagonal in a one-dimensional system or has a structure of block tridiagonal matrices for high spatial dimensions, one may develop a direct fast method to solve the linear equation (4) or (6). For a one-dimensional system, the Thomas algorithm [26] may be carried out directly. For two- or three- dimensional systems, the Alternating Direction Implicit (ADI) method [26] for direction splitting may be incorporated with the Thomas algorithm or a similar fast algorithm in each direction for the development of fast solvers.

Similar to Newton’s method, calculation of the Jacobian matrix in AIIE may also become problematic for the systems involving many species with reaction terms that may not be smooth enough for differentiation. In such cases, the approximation of the Jacobian matrix or a Jacobian-free approach [22] may be adapted for further improvement of the AIIE type of method.

A typical FAS multigrid approach with the nonlinear Gauss-Seidel smoother usually results in divergence or convergence to a homogeneous solution. Although the FAS multigrid method with the AIIE smoother can guarantee the convergence to an inhomogeneous steady

state, it costs more CPU time than the AIIE method in our simulations. It is important to develop a cheaper, though still robust, smoother for FAS. Again, the difficulty here is to balance the computational efficiency and ability of obtaining pattern solutions.

The essence of the AIIE method, which combines the implicit Euler method and Newton's method in this paper, is the integration of an implicit temporal scheme and an inexact nonlinear solver along with an adaptive iterative "step" to solve steady state pattern for reaction-diffusion equations. To utilize the strength of various temporal schemes (e.g., implicit vs. explicit) and nonlinear solvers (e.g., Newton's method vs. other types), one can incorporate other temporal schemes with Newton's method, or implicit Euler with other nonlinear solvers, or two other temporal and iterative methods for designing new hybrid methods that are more robust and more efficient than AIIE in exploring spatial steady state patterns driven by complex reaction-diffusion equations.

## Acknowledgments

This work was partially supported by National Institutes of Health grant Nos. R01GM67247 and P50GM76516, (to Q.N.) and National Science Foundation grant Nos. DMS-0917492 (to Q.N.), DMS-0811272 and DMS-1115961 (to L.C.). L.C. is also partially supported by 2010–2011 UC Irvine Academic Senate Council on Research, Computing and Libraries (CORCL). M. W. was supported by the China Scholarship Council. This research has been supported in part by the Mathematical Biosciences Institute and the National Science Foundation under grant DMS 0931642 (to W.-C. L.).

## References

1. Baker RE, Gaffney EA, Maini PK. Partial differential equations for self-organization in cellular and developmental biology. *Nonlinearity*. 2008; 21:R251–R290.
2. Epstein IR, Bansagi T, Vanag VK. Tomography of reaction-diffusion microemulsions reveals three-dimensional Turing patterns. *Science*. 2011; 331:1309–1312. [PubMed: 21310963]
3. Jilkine A, Edelstein-Keshet L. A comparison of mathematical models for polarization of single eukaryotic cells in response to guided cues. *PLoS Computational Biology*. 7:e1001121. [PubMed: 21552548]
4. Murray, JD. *Mathematical Biology*. 3. Springer Verlag; New York: 2002.
5. Park HO, Bi EF. Central roles of small gtpases in the development of cell polarity in yeast and beyond. *Microbiology and Molecular Biology Reviews*. 2007; 71:48–96. [PubMed: 17347519]
6. Pearson JE. Complex patterns in a simple system. *Science*. 1993; 261:189–192. [PubMed: 17829274]
7. Dillon R, Maini PK, Othmer HG. Pattern formation in generalized Turing systems I. Steady-state patterns in systems with mixed boundary condition. *Journal of Mathematical Biology*. 1994; 32:345–393.
8. Maini PK, Myerscough MR. Boundary-driven instability. *Applied Mathematics Letters*. 1997; 10(1):1–4.
9. Turing AM. The chemical basis of morphogenesis. *Philos Trans R Soc London, Ser B*. 1952; 237:37–72.
10. Goryachev AB, Pokhilko AV. Dynamics of Cdc42 network embodies a Turing-type mechanism of yeast cell polarity. *FEBS Letters*. 2008; 582:1437–1443. [PubMed: 18381072]
11. Lew DJ, Howell AS, Savage NS, Johnson SA, Bose I, Wagner AW, Zyla TR, Nijhout HF, Reed MC, Goryachev AB. Singularity in polarization: Rewiring yeast cells to make two buds. *Cell*. 2009; 139:731–743. [PubMed: 19914166]
12. Meinhardt, H. *Models of Biological Pattern Formation*. Academic Press; London: 1982.
13. Stephenson LE, Wolkind DJ. Weakly nonlinear stability analyses of one-dimensional Turing pattern formation in activator-inhibitor/immobilizer model systems. *Journal of Mathematical Biology*. 1995; 33:771–815.

14. Kolokolnikov T, Wei J. On ring-like solutions for the gray-scott model: Existence, instability and self-replicating rings. *European Journal of Applied Mathematics*. 2005; 16(2):201–237.
15. Wei J, Winter M. Stability of spiky solutions in a reaction-diffusion system with four morphogens on the real line. *SIAM Journal on Mathematical Analysis*. 2010; 42(6):2818–2841.
16. Cox SM, Matthews PC. Exponential time differencing for stiff systems. *Journal of Computational Physics*. 2002; 176(2):430–455.
17. Kassam AK, Trefethen LN. Fourth-order time-stepping for stiff PDEs. *SIAM Journal on Scientific Computing*. 2005; 26(4):1214–1233.
18. Nie Q, Wan FYM, Zhang YT, Liu XF. Compact integration factor methods in high spatial dimensions. *Journal of Computational Physics*. 2008; 227:5238–5255. [PubMed: 19809596]
19. Nie Q, Zhang Y, Zhao R. Efficient semi-implicit schemes for stiff systems. *Journal of Computational Physics*. 2006; 214:521–537.
20. Ruuth SJ. Implicit-explicit methods for reaction-diffusion problems in pattern formation. *Journal of Mathematical Biology*. 1995; 34:148–176.
21. Page KM, Maini PK, Monk NAM. Complex pattern formation in reaction-diffusion systems with spatially varying parameters. *Physica D*. 2005; 202:95–115.
22. Kelley, CT. *Iterative Methods for Linear and Nonlinear Equations*. SIAM; Philadelphia: 1995.
23. Brandt A. Multi-level adaptive solutions. *Mathematics of computation*. 1977; 31(138):333–390.
24. Briggs, WL.; Henson, VE.; McCormick, SF. *A Multigrid Tutorial*. SIAM; Philadelphia, Pennsylvania: 1987.
25. Xu J. A novel two-grid method for semilinear elliptic equations. *SIAM Journal on Scientific Computing*. 1994; 15:231–237.
26. Morton, KW.; Mayers, DF. *Numerical solution of partial differential equations*. Cambridge University press; 1995.
27. Stoer, J.; Bulirsch, R. *Introduction to Numerical Analysis*. 3. Springer Verlag; 2002.
28. Nocedal, J.; Wright, SJ. *Numerical Optimization*. 2. Springer Verlag; New York: 2002.
29. Levenberg K. A method for the solution of certain non-linear problems in least squares. *The Quarterly of Applied Mathematics*. 1944; 2:164–168.
30. Marquardt D. An algorithm for least-squares estimation of nonlinear parameters. *SIAM Journal on Applied Mathematics*. 1963; 11:431–441.
31. Chen, L. Technical Report. University of California; Irvine: An integrated finite element methods package in MATLAB.
32. Koch AJ, Meinhardt H. Biological pattern formation: from basic mechanisms to complex structures. *Reviews of Modern Physics*. 1994; 66:1481–1507.
33. Bhatia, R. *Fourier Series*, The Mathematical Association of America. 2004.



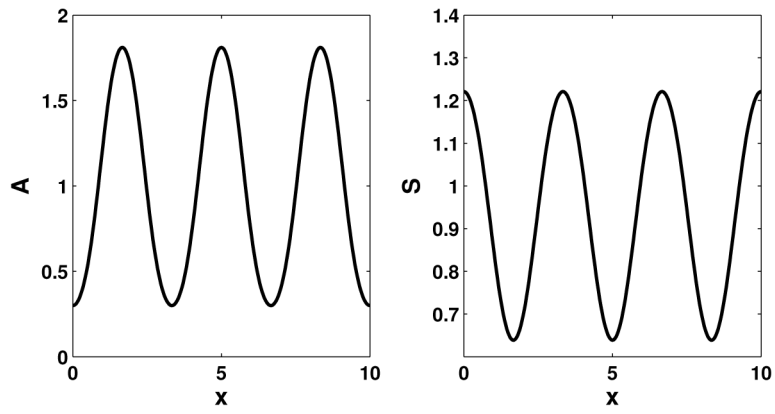


**Figure 1.** A typical inhomogeneous steady state pattern for the system (8) in a one-dimensional domain. The parameters for this case are  $D=0.1$ ,  $\rho=0.01$ , and  $\mu=1$ .

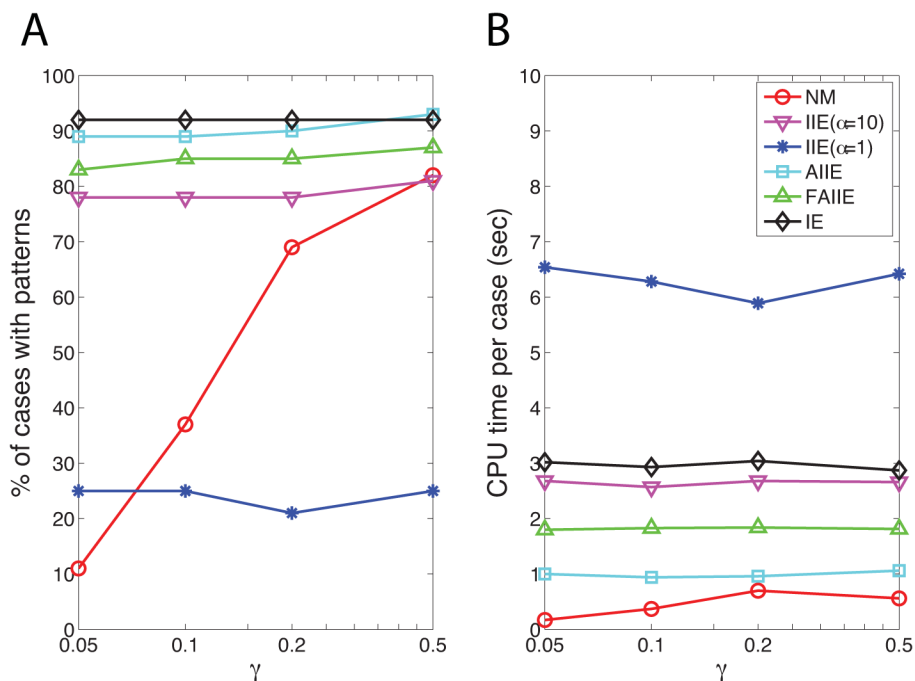


**Figure 2.** Comparisons of five different methods for solving system (8) in a one-dimensional domain. (A): The percentage of the simulations that converge to inhomogeneous steady state patterns as a function of the magnitude of the perturbation in the initial guess. (B): CPU time for simulating one set of parameters as a function of the magnitude of the perturbation acted on initial guess. The percentage and CPU time of the simulations at each marker are calculated within 100 random sample sets of parameters chosen from the ranges (12).

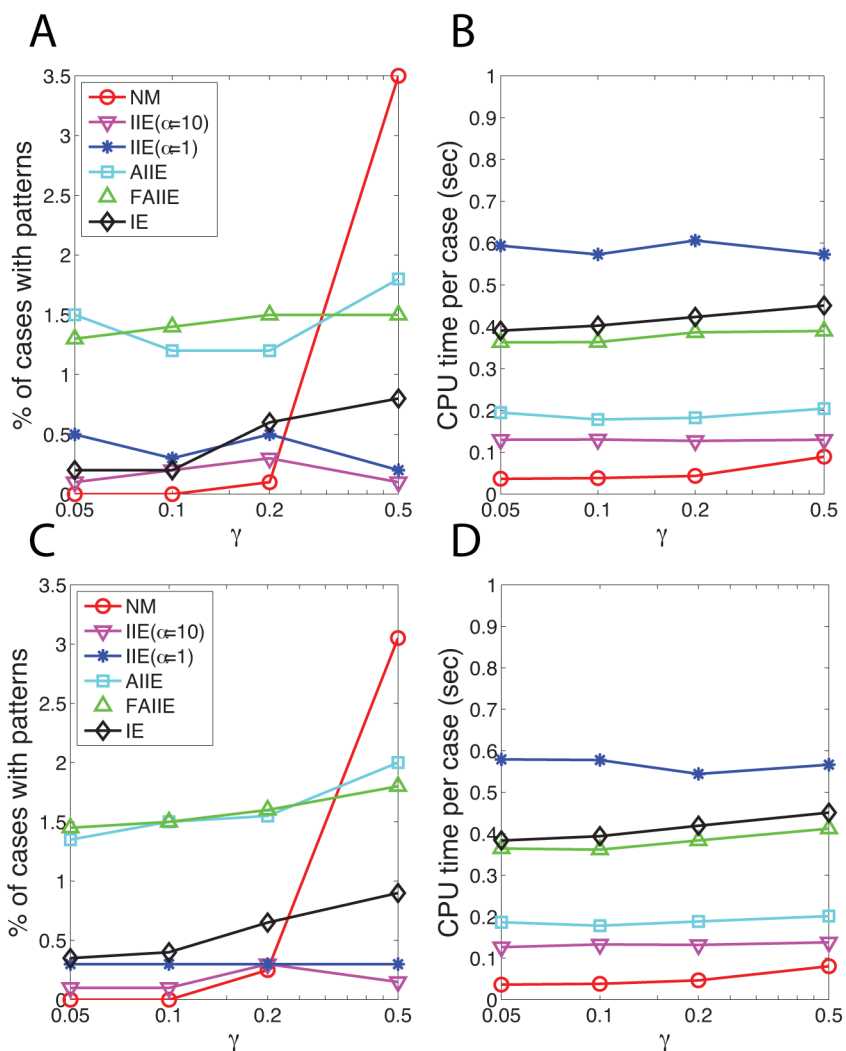


**Figure 3.** Comparisons of five different methods for solving system (14) in a one-dimensional domain. (A,C): The percentage of the simulations which converge to inhomogeneous steady state patterns as a function of the magnitude of the perturbation in the initial guess. (B,D): CPU time for simulating one set of parameters as a function of the magnitude of the perturbation acted on initial guess. The simulations at each marker in (A,B) and (C,D) are calculated within 1,000 and 2,000 random sample sets of parameters, respectively. All the parameters are chosen from the ranges (16).

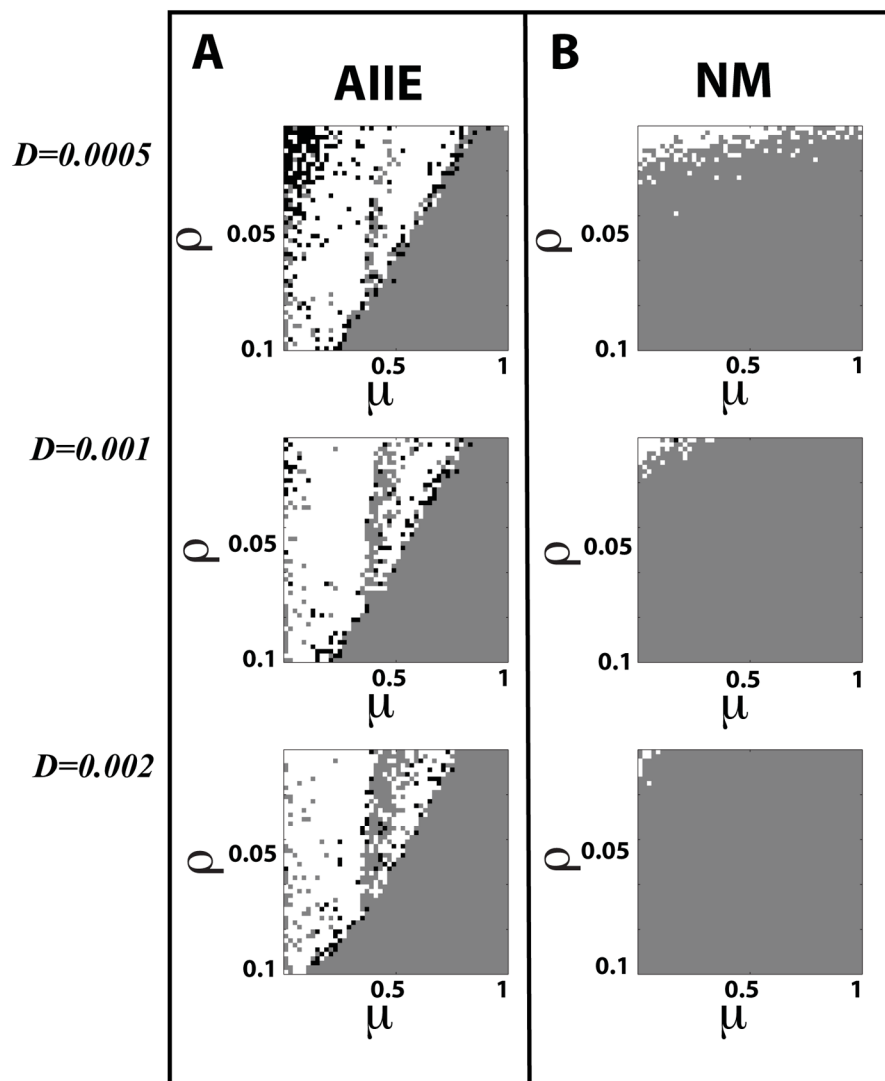


**Figure 4.** Comparison of AIIE and NM using *small* perturbation acted on initial guess ( $\gamma = 0.1$ ) for the robustness of convergence to an inhomogeneous pattern for solving system (14) in a one-dimensional domain. (A) AIIE. (B) NM. Grey: Convergence to a homogeneous steady state; White: Convergence to an inhomogeneous pattern; Black: Non-convergence for a tolerance of  $10^{-7}$  and a maximal iteration number of 1,000.

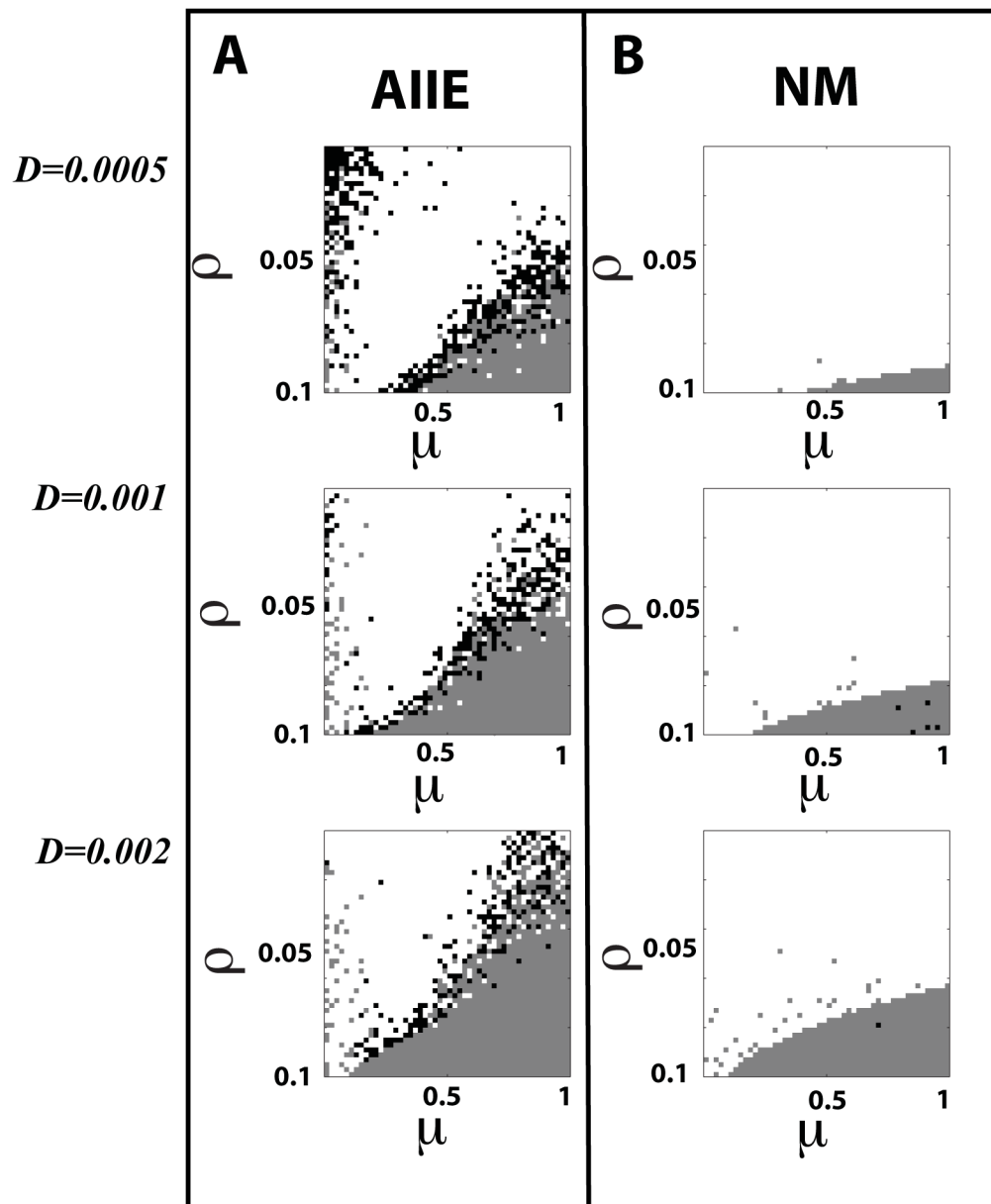


**Figure 5.** Comparison of AIIE and NM using a *larger* perturbation acted on initial guess ( $\gamma = 0.5$ ) for the robustness on converging to an inhomogeneous pattern for solving system (14) in a one-dimensional domain. (A) AIIE. (B) NM. Grey: Convergence to a homogeneous steady state; White: Convergence to an inhomogeneous pattern; Black: Non-convergence for a tolerance of  $10^{-7}$  and a maximal iteration number of 1,000.

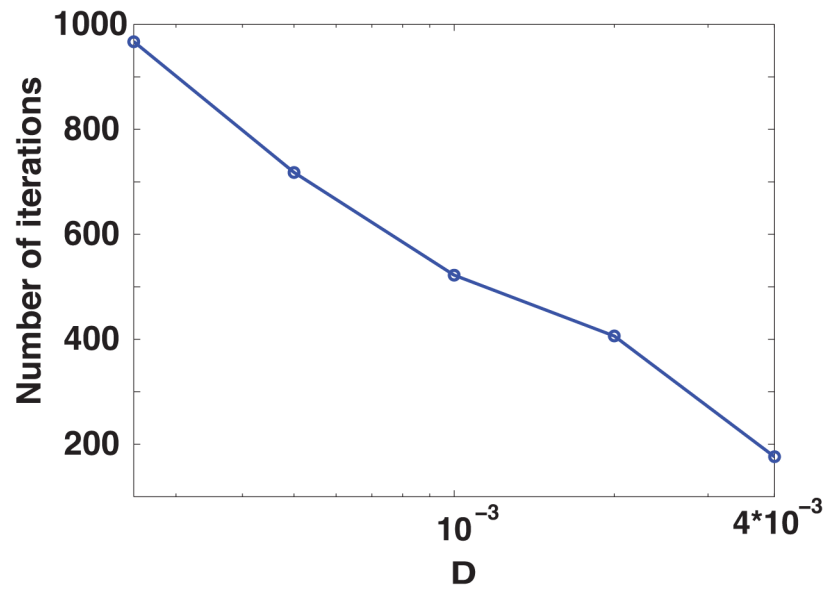


**Figure 6.** The number of iterations for AIIE to converge vs. the diffusion coefficient  $D$ . All the simulations have the same initial guess and the fixed parameters:  $J = 10$ ,  $\mu = 1$  and  $\rho = 0.1$

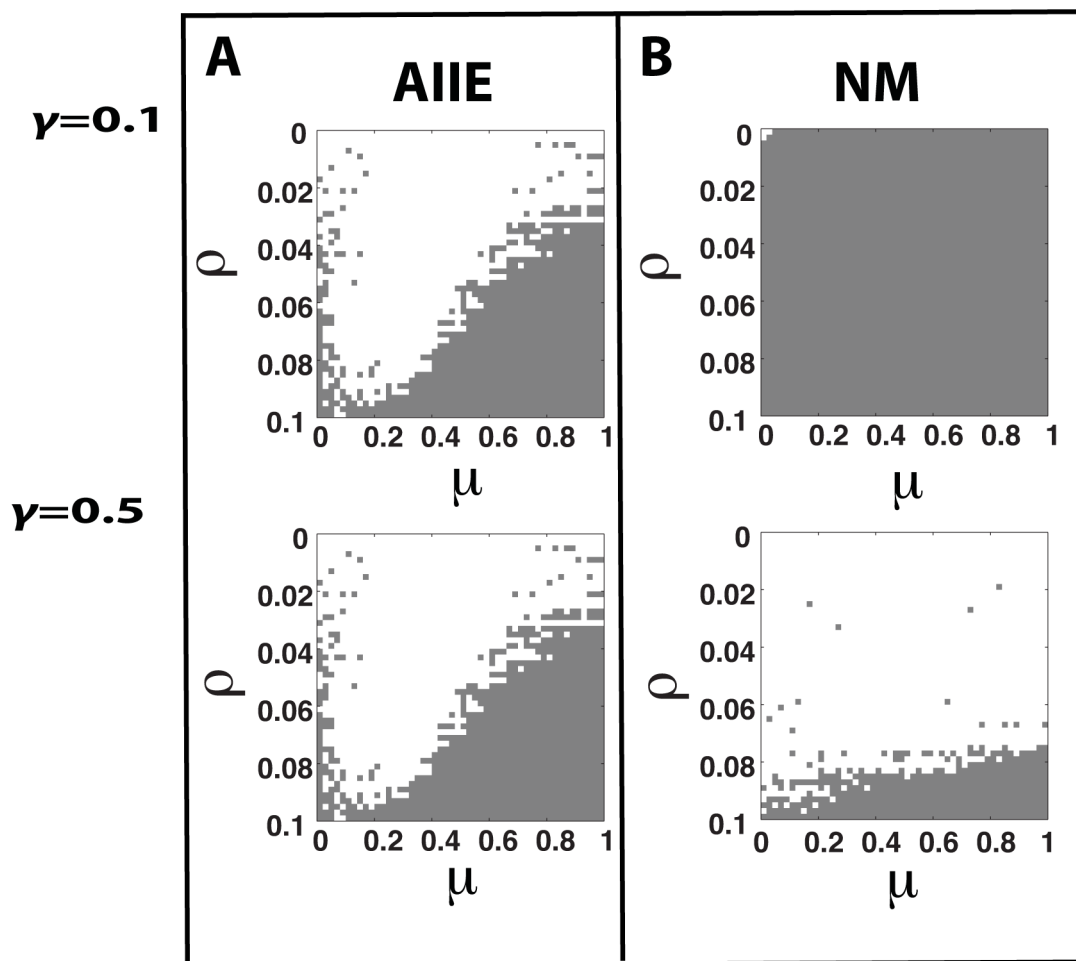


**Figure 7.**

Comparison of AIIE and NM, when applied to a *two-dimensional* system (14), for the robustness of converging to an inhomogeneous pattern with two different magnitudes of perturbation of the initial guess. (A) AIIE. (B) NM. Grey: Convergence to a homogeneous steady state; White: Convergence to an inhomogeneous pattern; Black: Non-convergence for a tolerance of  $10^{-7}$  and a maximal iteration number of 1,000.

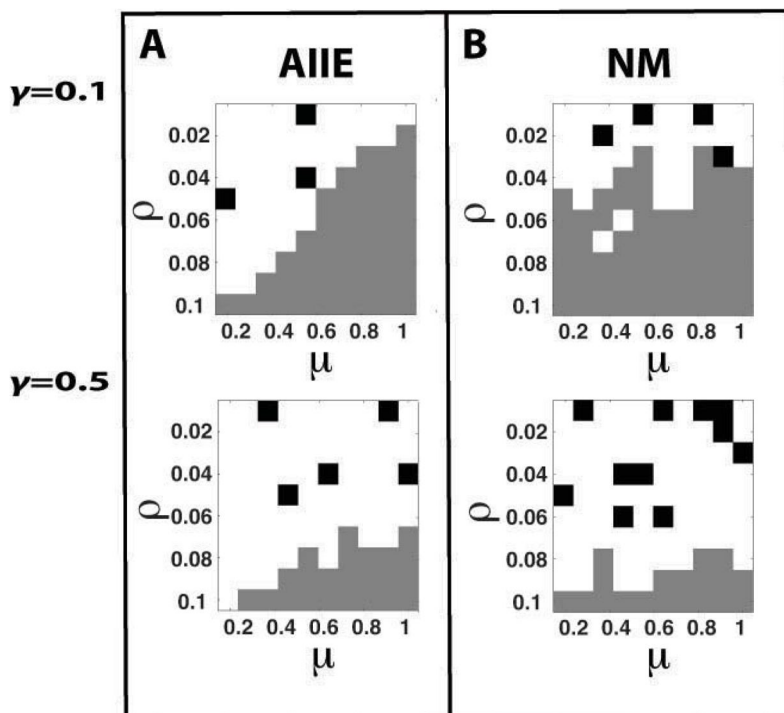


**Figure 8.** Comparison of AIIIE and NM, when applied to a *three-dimensional* system (14), for the robustness of converging to an inhomogeneous pattern with two different magnitudes of perturbation of the initial guess. (A) AIIIE. (B) NM. Grey: Convergence to a homogeneous steady state; White: Convergence to an inhomogeneous pattern; Black: Non-convergence for a tolerance of  $10^{-7}$  and a maximal iteration number of 1,000.



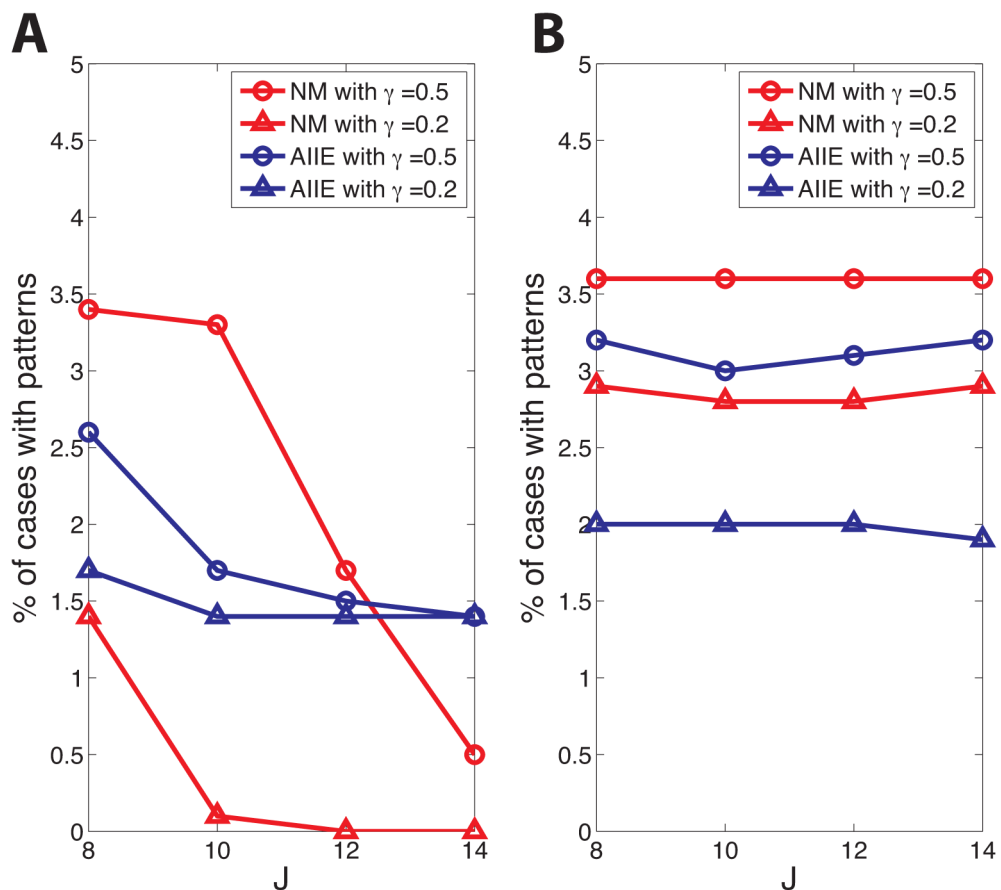


**Figure 9.** The percentage of the simulations that converge to inhomogeneous steady state patterns as a function of the spatial level  $J$  (number of spatial point  $N = 2^J + 1$ ). (A): With initial guess of form (17). (B): With initial guess linearly interpolated from the initial guess formed on  $J = 6$  coarse grid. The percentage of the simulations at each marker is calculated within 1,000 random sample sets of parameters chosen from the ranges (18).

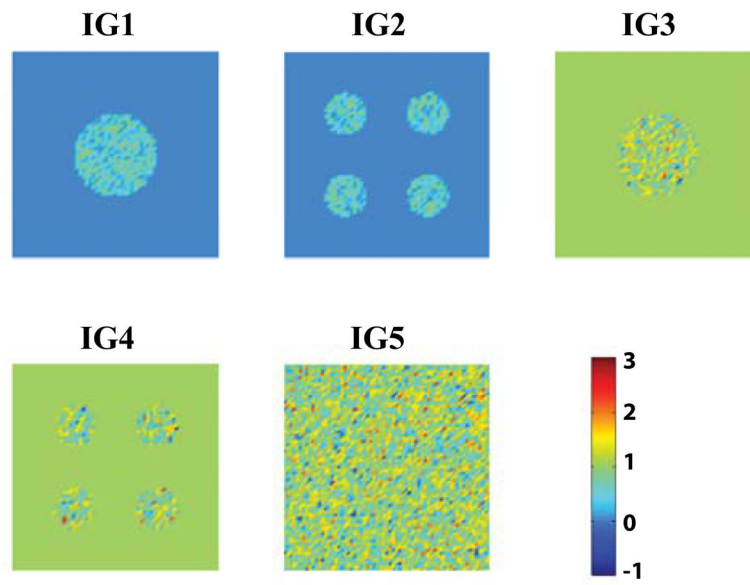


**Figure 10.** Five different sets of initial guesses used for spatial resolution refinement tests.

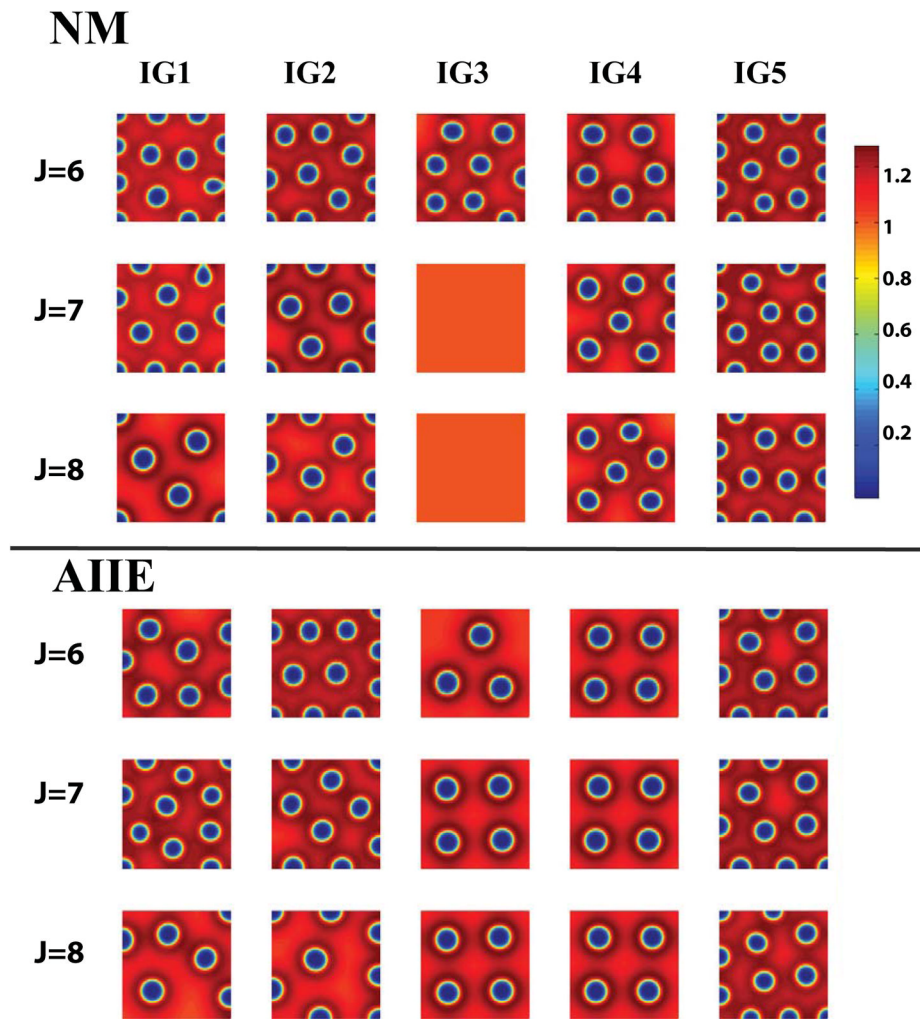


**Figure 11.** Two-dimensional patterns at three different spatial resolutions of AIIE and NM for solving system (14). All the simulations have a tolerance of  $5 \times 10^{-4}$  within 1,000 iterations.  $D=0.01$ ,  $\rho=0.01$  and  $\mu=0.5$ .

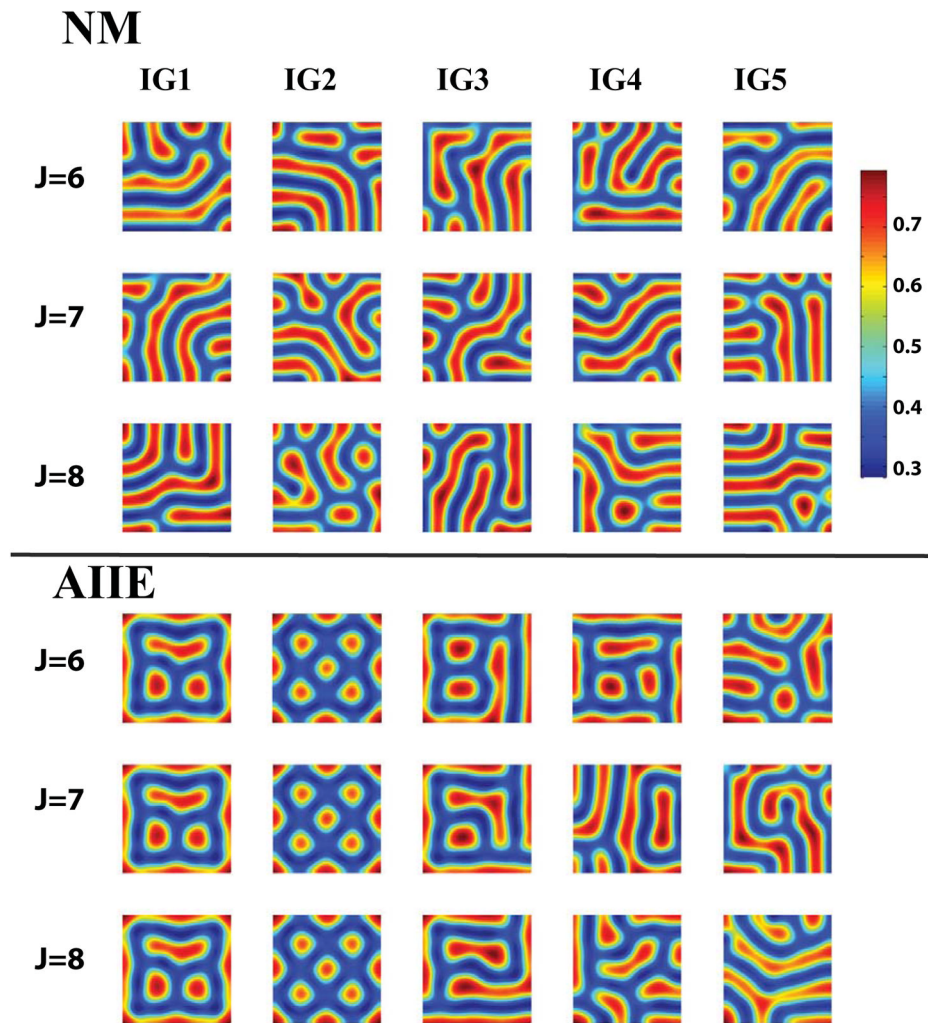


**Figure 12.** Two-dimensional patterns at three different spatial resolutions of AIIE and NM for solving system (22). All the simulations have a tolerance of  $5 \times 10^{-4}$  within 1,000 iterations.  $D_A = 0.01$ ,  $D_S = 0.005$ ,  $\rho = 0.04$  and  $k = 0.06$ .

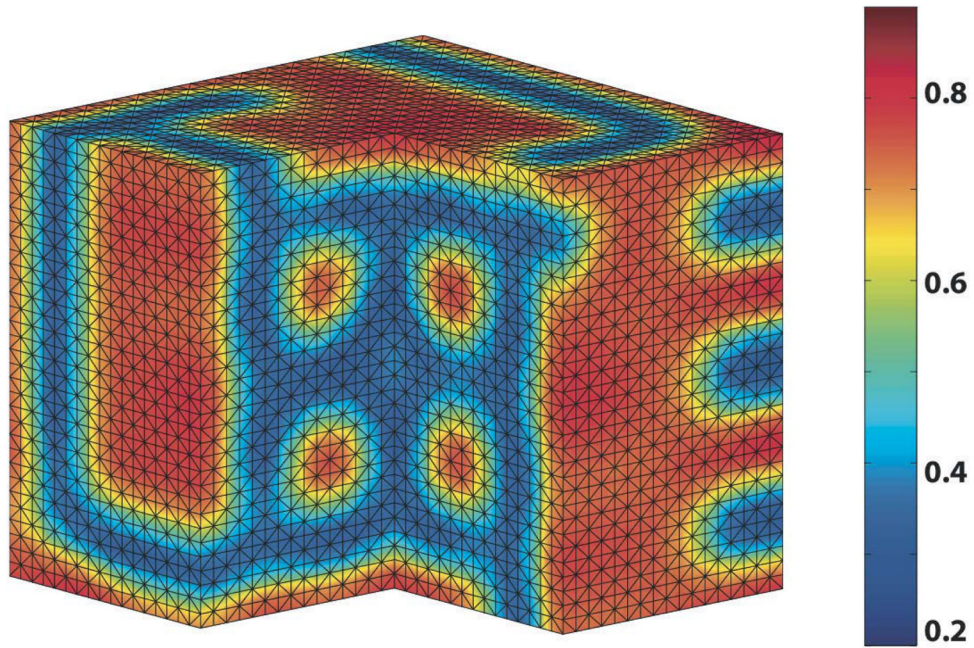


**Figure 13.** A three-dimensional pattern computed by AIIE for system (22) with initial guess of form IG1 and a tolerance of  $10^{-4}$ .  $D_A = 0.01$ ,  $D_S = 0.005$ ,  $\rho = 0.04$  and  $k = 0.06$ .